Properties of Single-Walled Carbon Nanotube-Based Poly(phenylene vinylene) Electroluminescent Nanocomposites

Mansour K. AbdulBaki,[1] Andrew Tangonan,[2] Rigoberto C. Advincula,[2] T. Randall Lee,[2] Ramanan Krishnamoorti[1,2]

[1]Department of Chemical & Biomolecular Engineering, University of Houston, Houston, Texas 77204

[2]Department of Chemistry, University of Houston, Houston, Texas 77204

Correspondence to: R. Krishnamoorti (E-mail: ramanan@uh.edu)

Received 20 September 2011; revised 6 November 2011; accepted 7 November 2011; published online 29 November 2011
DOI: 10.1002/polb.23007

ABSTRACT: Devices with varying concentrations of single-walled carbon nanotubes (SWNTs) dispersed in three derivatives of poly(*p*-phenylene vinylene) are prepared, and their electroluminescent properties evaluated. Increasing the concentration of SWNTs improves the electrical conductivity of the nanocomposites. However, an undesired increase in the electroluminescence (EL) turn-on voltage is observed for the hybrids, possibly due to photoluminescence quenching of excitons by the SWNTs. At relatively low concentrations of SWNTs, there is an increase in the EL lifetime; in contrast, at relatively high concentrations of SWNTs, due to photoluminescence quenching by the nanotubes, significant reduction in brightness and faster degradation of the EL performance of the devices is observed. © 2011 Wiley Periodicals, Inc. J Polym Sci Part B: Polym Phys 50: 272–279, 2012

KEYWORDS: carbon nanotubes; conducting polymers; exciton quenching; MEH-PPV; optoelectronics; organic light-emitting diodes

INTRODUCTION Advances in the fabrication, characterization, processing, and performance of light-emitting devices employing organic and polymeric materials are critical to the development of next-generation photovoltaic cells, conductive coatings, optoelectronics, and flat-panel displays.[1–3] Czerw et al.[4] have studied the failure modes of polymeric light emitting diodes (LEDs) in efforts to understand interfacial issues arising from fabrication techniques as well as how device lifetimes are limited by material degradation, such as the delamination of layers (the cathode), the formation of gas bubbles, and the carbonization of polymers.[4,5] Although it is known that protective encapsulation increases device-lifetimes by orders of magnitude and inhibits the growth and formation of non-emissive dark spots,[6] methods to shelter the active device from moisture add cost and complexity to fabrication steps and still fail to completely eliminate degradation.[4,6] In this context, it has been suggested that the incorporation of nanomaterials into conducting polymers, used as the light-emitting layer in LEDs, might lead to significant improvement in device performance.[2,7] Single-walled carbon nanotubes (SWNTs) are promising candidates due to their exceptional thermal and electrical properties along with their interesting chemical properties. SWNT-based polymer nanocomposites have been shown to exhibit considerable enhancement in electrical conductivity without loss of chemical or thermal stability.[3]

Poly(*p*-phenylene vinylene)s (PPVs) have gained popularity among conjugated polymers due to their physical and optical properties (e.g., electrical conductivity and electroluminescence (EL)) and because they can be readily synthesized in high purity and with high molecular weights.[8] PPVs also lend themselves to side-chain functionalization, allowing one to tailor the electrical, optical, and macroscopic properties of the polymer chain along with the solubility in various organic solvents. More precisely, side-chain functionalization provides control over conductivity, emission wavelength, and the solubility of derivatives, enhancing the attractiveness of these materials and facilitating their processing in the manufacture of microelectronics and optoelectronic devices.

One of the most widely studied polymers in this class is poly[4-methoxy-1-(2′-ethylhexyloxy)-*p*-phenylene vinylene], (MEH-PPV) (Fig. 1). The long-branched ethylhexyloxy substituent on the aromatic ring gives enhanced solubility in organic solvents, leading to easier handling and processing. To generalize the results and to illustrate the inclusion of SWNTs, we chose to study other PPV derivatives as well, including poly[4-methoxy-1-(2′-ethylhexyloxy)-*p*-phenylene cyanovinylene] (MEH-PPCNV) and poly(1,4-dihexyloxy)-*p*-phenylene cyanovinylene) (DH-PPCNV), which are also shown in Figure 1. These derivatives are also examples of how the solubility and color of this class of polymers can be

Additional Supporting Information may be found in the online version of this article

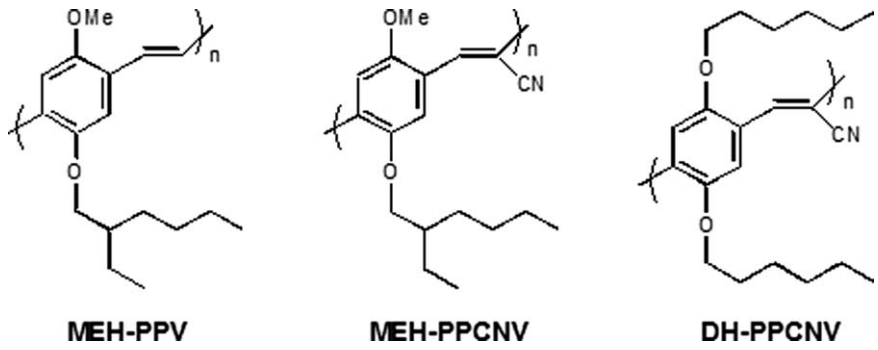

FIGURE 1 Structures of the repeat units of (a) poly[4-methoxy-1-(2′-ethylhexyloxy)-*p*-phenylene vinylene] (MEH-PPV), (b) poly[4-methoxy-1-(2′-ethylhexyloxy)-*p*-phenylene cyanovinylene] (MEH-PPCNV), and (c) poly(1,4-dihexyloxy)-*p*-phenylene cyanovinylene) (DH-PPCNV).

manipulated. MEH-PPV is orange in color and soluble in tetrahydrofuran (THF) and *N*,*N*-dimethylformamide (DMF), but less soluble in ε-caprolactone (ECL). In contrast, the cyano-containing MEH-PPCNV is bright yellow and readily soluble in both DMF and ECL, while the DH-PPCNV is dark red-orange and is slow to dissolve in DMF and almost completely insoluble in ECL. Additionally, the presence of the cyano groups in the latter derivatives decreases the electron density along the polymer backbone and can reduce the barrier to electron injection in light-emitting devices.[9]

Considerable obstacles along the path to harnessing the properties of carbon nanotubes in polymer nanocomposites are their lack of dispersibility in solvents and polymers[10–12] and their strong affinity for one another.[12–15] SWNTs are relatively inert and highly insoluble due to their sp^2 hybridized structure, a strong hydrophobicity, $\pi-\pi$ stacking, relatively strong van der Waals interactions,[16,17] and their high aspect ratio. Enhanced dispersion and dispersibility/or dissolution have been achieved using surfactant-assisted methods[18,19] and covalent sidewall functionalization of the nanotubes.[20,21] The addition of surfactants to solubilize nanotubes introduces a third-component to polymer nanocomposites that can lead to plasticization of the polymer and the creation of a complicated interface between the polymer and the nanotube. On the other hand, covalent functionalization offers the possibility of attaching functional groups or other molecules to the nanotubes and therefore leads to enhanced compatibility with polymers.[10,20,22–24] However, covalent chemical modification interrupts the extended π-conjugation of nanotubes and creates defect sites, effectively reducing their electrical conducting properties, tensile strength, and overall stability. While successful functionalization of the walls of carbon nanotubes might find use in certain technological applications, these strategies will compromise those applications that require high electrical conductivity,[10] high strength, and long-term stability. Thus, the focus here is on the effects of SWNTs in electroluminescent polymer systems by simple solvent assisted dispersion of the nanotubes.

Previous work in similar nanocomposite systems has shown the ability to improve, systematically, the performance of polymer-based devices using dilute concentrations of SWNTs (i.e., 0.01–0.1 wt %).[25–27] We show here that these benefits do not translate to higher concentration SWNT-PPV nanocomposites, possibly due to the formation of an electrically percolated network of SWNTs and/or due to photoluminescence quenching in these hybrid materials.

EXPERIMENTAL

Reagents

All solvents and reagents were commercially available and used as received unless otherwise stated. For the synthesis of MEH-PPV, the monomer α,α'-dibromo-2-methoxy-5-(2-ethylhexyloxy)xylene was synthesized using a literature procedure.[8] The reagent 4-methoxyphenol was purified by sublimation. The THF and DMF used in the polymerization reactions were freshly distilled from sodium/benzophenone, and calcium hydride, respectively. MEH-PPV was prepared as previously reported.[28] MEH-PPCNV and DH-PPCNV were used as received from Polyorganix, Inc. An aqueous solution of poly(3,4-ethylenedioxythiophene):poly(styrenesulfonate) (PEDOT:PSS) was obtained from Bayer Corporation. Solvents used in preparing the composites were analytical grade and used as received from Sigma-Aldrich chemical company. Prepurified SWNTs were obtained from Carbon Nanotechnologies Inc., and used as received without further modification.

Nanocomposite Preparation and Characterization

The SWNT dispersions were prepared by ultrasonication in the chosen solvents, DMF and ECL, for 3 h using a NEY ULTRAsonik 19H sonicator. The dispersions were then centrifuged to remove any remaining aggregates. In the case of the MEH-PPV composites, centrifugation at an acceleration of 5600*g* gave a supernatant dispersion with a final concentration of 0.025 mg SWNTs/mL DMF. Subsequent addition of 1, 3, or 7 mL of this suspension to 5 mL solutions of 3.45 mg MEH-PPV/mL THF yielded final composites with loadings of 0.1, 0.4, and 1.0 wt % SWNTs, respectively. For the MEH-PPCNV materials, the solutions were centrifuged at 1000*g* and a supernatant dispersion of 0.066 mg SWNT/mL DMF. The addition of 1, 3, and 7 mL of this suspension to 3 mL solutions of 3.33 mg PPV/mL DMF yielded final composites with loadings of 0.7, 1.9, and 4.4 wt % SWNTs, respectively.

Final composite concentrations of SWNT dispersed by ECL gave loadings of 0.1, 0.3, and 0.7 wt % SWNTs in DH-PPCNV.

To evaluate the dispersion of SWNTs from their preferred bundled state, UV–vis–NIR spectra were examined for each dispersion solution using a JASCO V-570 UV–vis–NIR spectrophotometer. Solutions with dispersed SWNTs show characteristic peaks between 400 and 1400 nm wavelengths.[19,29] These absorption bands arise from the van Hove singularities that become apparent when SWNTs are individualized due to their high density of energy states. SWNTs present in bundles do not show van Hove absorption peaks; instead revealing a monotonically decreasing absorption spectrum as the wavelength increases.[30]

Dispersions of the SWNTs were then added in systematically varying amounts to stirred solutions of each polymer to obtain different concentrations of SWNTs. Efforts were made to have roughly the same polymer concentration in each solution and therefore roughly equal viscosity across the samples, leaving only the effects due to the varying SWNT concentrations on overall solution properties. UV–vis–NIR spectra were collected for the polymer composite solutions as well, and the continued good dispersion of the SWNTs in these polymer solutions was confirmed.

Photoluminescence spectra were acquired by adding an equal number of drops of a nanotube dispersion of the polymer solutions onto cleaned glass slides. The droplets were then spin coated into thin films at 1000 RPM using a Speedline Technologies P6204 spin-coater so that the data would reflect those at the physical state of the working devices. The photoluminescent spectra were collected with a Perkin–Elmer LS45 luminescence spectrometer. The excitation wavelength of 460 nm was chosen after observing an absorption maximum at 454 nm.

Glass slides coated with indium tin oxide (ITO) were obtained from SPI Supplies with an initial surface resistance of $\sim$15 ohms/square. After cutting into 1 $\times$ 1 inch squares, the ITO pieces were sonicated sequentially for 15 min in an aqueous 2% surfactant solution, then in water, followed by acetone, and finally in isopropanol. The ITO was then covered with two strips of Scotch brand tape to serve as a mask against acid etching, which was conducted by placing the slides in a solution of 1:1 H_2O and HCl for 30 min. After etching, the substrates exhibited a surface resistance of 23–25 ohms/square and were again sonicated for 15 min sequentially in DI water, acetone, and isopropanol. The substrates were then cleaned under an oxygen plasma for 5 min and then spin coated with PEDOT:PSS solution at 1000 RPM. After drying the PEDOT/PSS-coated substrates for 2 h in a vacuum oven at 50 °C, each of the polymers was then spin coated at 1000 RPM, maintaining a thickness of $\sim$100 nm, confirmed by contact atomic force microscopy (AFM) (Supporting Information Fig. S3). The substrates were then placed under vacuum at 50 °C for 1 h. Aluminum was thermally evaporated at $< 10^{-6}$ Torr using an Edwards E306 Thermal Evaporator. These procedures are shown in Supporting Information Figure S4. The active sections of the devices were then covered with an epoxy resin and allowed to dry so that these regions were shielded from oxygen and moisture during storage and device testing. This application of a sealant to the device is effective, although not as insulating as the additional glass pane used in a previous study by Burrows et al.[6] The devices were tested using a Keithley 236 source meter unit, a Hamamatsu photonics photomultiplier, and a self-written LabView® program. Current–Voltage–Luminescence (*I-V-L*) data were collected from 0 to 10 volts at steps of 0.1 volts and normalized by the active area of each LED section. EL lifetime measurements were collected under a constant potential of 6 volts and normalized by the maximum intensity of each run. Testing under a constant voltage as opposed to constant current density or EL intensity was determined to be the most relevant procedure as the potential difference across the device is what determines electron/hole injection and thus eventual exciton formation. Reproducibility of the electrical and optical output was high and a testament to the easy device fabrication method that allowed for many devices to be produced at once.

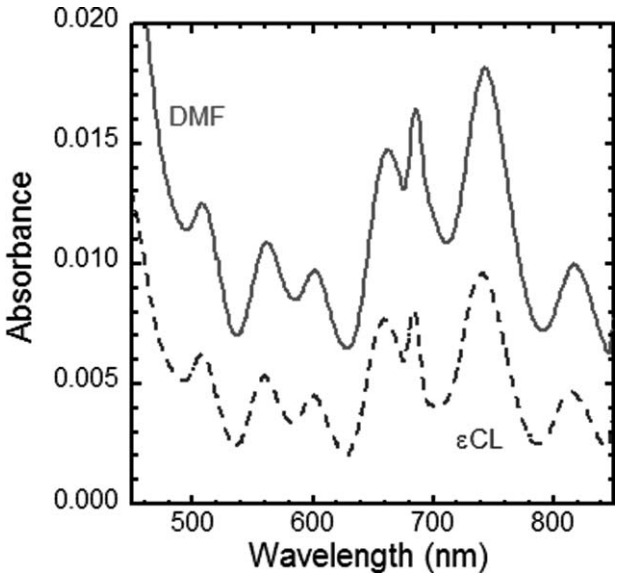

FIGURE 2 UV–vis–NIR absorption spectra for SWNT dispersions in DMF and ECL. These dispersions were subsequently mixed with polymer solutions to give nanocomposites after complete removal of the solvent.

RESULTS AND DISCUSSION

The UV–vis–NIR absorption spectra for SWNTs dispersed in DMF and ECL are shown in Figure 2. Sharp absorption bands corresponding to van Hove transitions in the 400–1400 nm wavelength range are easily discernable.[19,29] The absolute amounts of nanotubes dispersed in the two solvents are different, with the amount dispersed in DMF significantly larger than that in ECL, consistent with previous results.[13] Ausman et al. have shown that certain solvo-chemical properties are necessary though not sufficient for the dispersion of

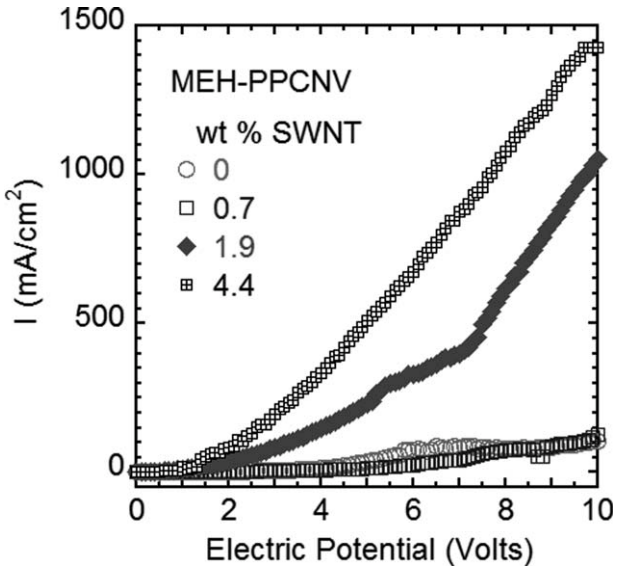

FIGURE 3 Current density (I) versus electric potential (V) for an ITO/PEDOT:PSS/PPV/Al OLED, where the PPV is MEH-PPCNV. Two features are readily observed for increasing nanotube concentration: reduced potentials for electrical turn-on ($V_I^{turn-on}$) and increased values of the slope of I versus V (beyond $V_I^{turn-on}$). Both features are consistent with a reduction in the electrical resistance of the device upon incorporation of SWNTs into the emissive PPV layer.

SWNTs.[13] In particular, solvents with high values for electron pair donicity (β), negligible values for the hydrogen bond donation parameter of Taft and Kamlet (α), and high values of the solvochromic parameter (π) have the best chance at being good dispersants for SWNTs. Thus, availability of a free electron pair (Lewis basicity) and the absence of hydrogen donors are key factors. The solvochromic parameter is an indication of the polarizability of a solvent. Among a large variety of solvents previously examined, those that contain amide groups, such as DMF and *N*-methylpyrrolidone (NMP), have been shown to be two of the best solvents for dispersing SWNTs.[13] In our work, dispersions in DMF show the sharpest van Hove peaks, corresponding to better dispersion of the SWNTs. Simply based on the optical density of the solutions, the dispersions in DMF were darker than the dispersions in ECL, which held fewer individualized SWNTs.

To measure the device performance and understand the influence of nanotube incorporation, the electroluminescent and photoluminescent properties of the nanocomposites were probed and compared to those of the pure polymers. A plot of current density as a function of applied potential is shown in Figure 3 for MEH-PPCNV and the SWNT-based MEH-PPCNV nanocomposites. The current density results for the three different polymers based nanocomposite suites are presented in Supporting Information Figure S5. An enhancement in electrical performance in the form of lower potentials for electrical turn-on, $V_I^{turn-on}$, is observed with increasing SWNT concentration. For pure MEH-PPCNV, the value of $V_I^{turn-on}$ is 3.3 V and drops to 2.5 V, 1.9 V, and 1.9 V for the 0.7, 1.9, and 4.4 wt % SWNT composites, respectively. Further, the slopes of the current density (I) versus voltage (V), beyond the $V_I^{turn-on}$ value, increase with increasing concentration of SWNTs. This slope, dI/dV, increases by factors of 3 and 7 for the 1.9, and 4.4 wt % SWNT composites, respectively. These two features of lowered value of $V_I^{turn-on}$ and increased dI/dV are likely due to the high conductivity of the SWNTs and the formation of nanotube-assisted conductive pathways in the devices.

To compare the different devices studied, we examined the current density at a constant potential of 6 V. At this voltage, the current density for the 0.7 wt % nanocomposite was similar to that of the unfilled MEH-PPCNV with the exception of a slightly lower value for the electrical turn-on voltage. However, the current density for the 1.9 and 4.4 wt % SWNT-polymer LEDs increased by factors of 4 and 9, respectively, over that of the pure polymer. Several separate devices were fabricated and all electrical tests gave similar results. A double log plot of I versus V (Supporting Information Fig. S8) revealed that the two more highly loaded devices are Ohmic, and the pure polymer and 0.7 wt % SWNT hybrid-based devices enter a space-charge limited conduction (SCLC) regime above 3.6 V and 5 V, respectively. As a whole, these data are consistent with a model in which the SWNTs reduce the electrical resistance of the devices, allowing for a higher current density through the material with the application of a lower operating voltage.

The EL turn-on voltage ($V_{EL}^{turn-on}$) and slope of the EL with respect to electrical potential, $d(EL)/d(V)$, were used as two measures of the electroluminescence performance of the device. If the nanotubes were to act only as conductors of electrons, then the values of $V_{EL}^{turn-on}$ should mirror the electrical activity in the devices, as it has with previous polymer-only devices we fabricated using the same methods.[31] We thus anticipate that the addition of SWNTs enhance the EL performance, with the emission of light occurring at lower electrical potentials. Figure 4 shows EL performance curves for MEH-PPCNV spun-cast from DMF with varying concentrations of SWNTs. The results of the EL measurements are inconsistent with the hypothesized trend. Although the electrical turn-on voltage ($V_I^{turn-on}$) decreases with increasing SWNT concentration, the EL turn-on voltage ($V_{EL}^{turn-on}$) increases with increasing SWNT concentration (see also Fig. 5). While the pure polymer exhibits the lowest value for $V_{EL}^{turn-on}$ at 3.7 V, those of the 0.7, 1.9, and 4.4 wt % nanocomposites increase to 4.7, 4.8, and 5.5 V, respectively.

These results, and similar results for the MEH-PPV and DH-PPCNV hybrids, indicate that the required potential to detect optical emission from the devices increases with increasing SWNT loading (Supporting Information Figs. S6 and S7). This behavior can perhaps be attributed to quenching by the increased nanoparticle inclusions, which causes the optical turn-on to appear at higher voltages where enough emission events are produced to overcome the SWNT

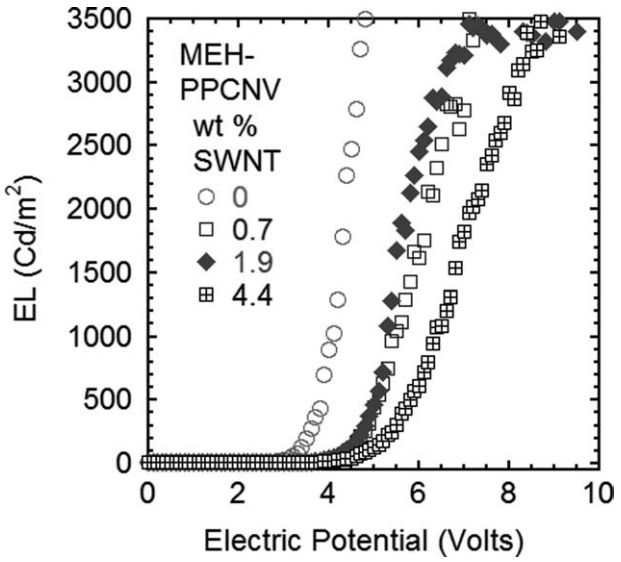

FIGURE 4 EL versus voltage for an ITO/PEDOT:PSS/PPV/Al OLED, where the PPV is MEH-PPCNV.

photoluminescence quenching barrier and be detected outside of the device. Furthermore, the formation of highly conductive SWNT nanoparticle-based conductive network pathways would effectively compete with the polymer for electron transport and also result in an alteration in the electrical field experienced by the polymer. Both of these possibilities are consistent with previous results showing trends of improvement in the EL turn-on voltage of devices using significantly lower SWNT concentrations in their composites,[25–27] where the quenching and formation of conductive network pathways may have been negligible. The dominant electronic interaction in polymer-nanotube composites has been shown to be the photo-induced polymer-to-SWNT electron transfer.[32–36] As such, changes in the efficiency of the produced devices arises from a competition between the improved exciton formation due to SWNT-enhanced electron mobility and the non-radiative decay at the SWNT–polymer junctions. Recent work has explored the influence of SWNTs on charge-carrier mobility in MEH-PPV[37] and found that while hole mobility is essentially unaffected, electron mobility increases nearly linearly with SWNT concentration. While the electrons in the nanocomposites travel through both the polymers and the SWNTs, the increase in mobility is attributed wholly to the SWNTs with the polymers acting as bridges between these more highly conductive pathways. Keeping the concentration of nanotubes below their contact percolation threshold could lead to improved electron mobility while guaranteeing that electrons move through the polymer at some point, thus continuing to allow for electron–hole recombination within the emissive layer of the device.

Another hypothesis could also rationalize the observed behavior at high SWNT concentrations. Above the contact percolation threshold of the SWNTs, it is plausible that the preferred electron pathway (that of lowest resistance) will be through the connected SWNT network. This connected network path of SWNTs limits the number of electrons available for recombination in the emissive layer and eliminates the need for the polymer bridges to complete the electrical network. On the other hand, at low SWNT concentrations the observed decrease in EL with increased SWNT loading at any particular current may result from a decrease in exciton formation or from an increase in non-radiative exciton decay. An increase in the non-radiative exciton decay above some SWNT percolation threshold should lead to an increase in the photocurrent,[38] which some recent work has reported is the case.[38,39] The increase in the photocurrent is most likely due to the high population of the SWNTs and the "electron expressways" that interrupt exciton pathways supporting charge carrier separation as well as allowing little chance for exciton formation to occur. In fact, while both Xu et al.[39] and Mulazzi et al.[38] have shown increased photocurrent, Mulazzi's *in situ* polymerization in the presence of SWNTs led to shorter PPV polymer lengths and directly demonstrated that photoluminescence only occurs if the excitations remain contained on short segments of PPV or are allowed to migrate on longer segments without encountering the network of SWNTs. Below the percolation of the SWNTs, where exciton formation is still significant, the effect of charge-carrier separation at the SWNT–polymer interface is more likely to be on par with the effect of electrons preferentially moving along the SWNTs when they are encountered. While Woo et al. have demonstrated hole-trapping by SWNTs,[40,41] Fournet

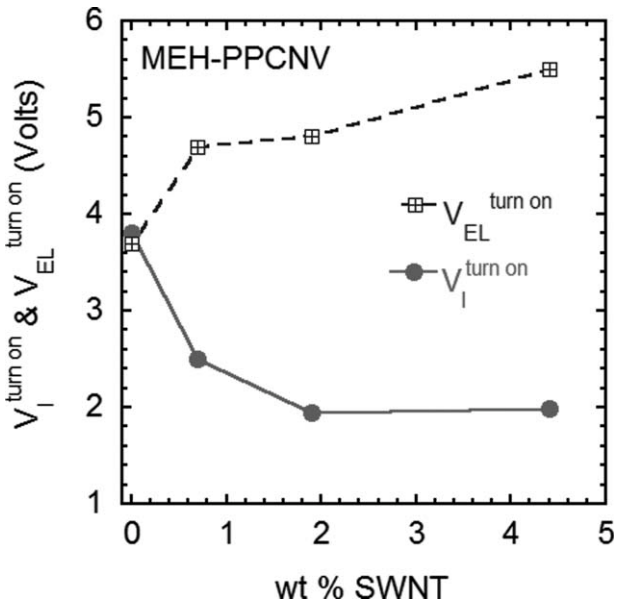

FIGURE 5 The current and electroluminescent turn-on voltages with respect to SWNT loading for an ITO/PEDOT:PSS/PPV/Al OLED, where the PPV is MEH-PPCNV. The turn-on current is reduced with the addition of SWNTs. The increase in potential required for EL turn-on hints at the possibility of photon quenching by the SWNTs.

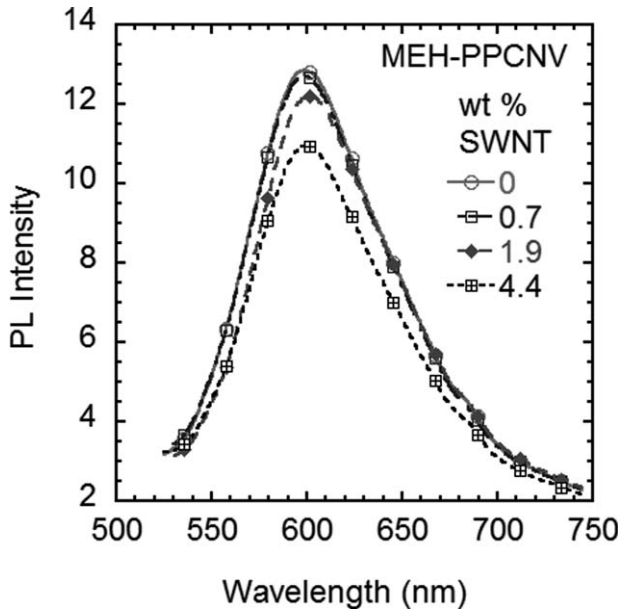

FIGURE 6 Photoluminescence spectra for various concentrations of SWNTs in MEH-PPCNV thin films on glass. The intensity at 600 nm for each sample plotted with respect to SWNT concentration shows a linear relationship. The excitation wavelength used here is 460 nm.

et al.[25] have suggested that, above the percolation threshold, the drop in EL can be rationalized by a change in the hole conduction pathway from that of the polymer alone to the combined CNT-polymer networks. Conduction via the latter pathway would decrease the likelihood of exciton formation in the emissive layer in a manner analogous to that mentioned for the electrons.

Photoluminescence spectra of thin films made from MEH-PPCNV on glass with varying concentrations of SWNTs are shown in Figure 6. Solvent was added to each solution before spin coating to normalize the polymer concentration and leave the amount of SWNT as the only manipulated variable between the samples. While the emission wavelength of the films remains unaffected, the photoluminescence at 600 nm decreases linearly with increasing SWNT concentration, further lending support to the idea that the behavior observed during optical testing of the devices arises from increased SWNT concentrations inducing other non-radiative recombination channels and mechanisms. Similar quenching data has been reported in the literature.[32–34,36,38,42] While we have taken great care to ensure identical polymer concentration and similar conditions for the development of the films for photoluminescence testing, the quantitative interpretation of the luminescence data and attributing them to specific mechanisms is beyond the scope of the measurements described here. Future experiments aimed at elucidating the fluorescence character of the SWNTs may include the evaluation of absorbance and fluorescence of each component, measurement of any Stokes shift, and fluorescence lifetimes to interpret the Förster resonance energy transfer (FRET) mechanism.

Another important property of polymer-based LEDs is their device lifetimes. A constant voltage of 6 V was applied to the devices while monitoring the time dependence of the electroluminescent intensity, wherein the devices were sealed from oxygen and moisture exposure by an epoxy layer. While fullerenes cannot behave as the metal nanoparticles of Hale et al.[7] which are tuned to resonate with the polymer's triplet state, both C_{60} and SWNTs have a high electron affinity and can thus behave as radical scavengers and are therefore expected to increase device lifetimes.[43] The oxidative degradation of polymers can occur via radical chain reactions of both alkyl and alkylperoxyl radicals. It follows then, that these routes of degradation may be inhibited by the presence of SWNTs, which are capable of trapping the radicals, leading to an antioxidant effect on the polymer.[9,13,43,44] On examining the results of lifetime testing in Figure 7, it can be observed that the addition of SWNTs to PPVs, here MEH-PPV, noticeably improves the lifetime performance of the devices. After 1 min, the brightness of the 0.1 wt % SWNT-based MEH-PPV nanocomposite devices is at 67% of its original intensity while the value is reduced to 25% and 9% for the 0.4 and 1.0 wt % SWNT devices, respectively. On the other hand, for the pure polymer-based device the remaining brightness was 3.4%. After 2 min, the pure polymer-based and 0.1, 0.4, and 1.0 wt % loaded SWNT nanocomposite-based devices retain 1.1, 33, 8.7, and 3.1% of their original brightness. These results indicate that the intermediate concentration of the SWNTs leads to longer lifetimes, with the lifetimes for the high concentration nanocomposites still exceeding that of the pure polymer. This observed maximum in the brightness retained and consequently apparent lifetime is thought to occur because of compensatory effects with increasing SWNT concentration. The dispersed SWNTs are thought to improve the degradation resistance of the polymers due to the trapping of radicals noted previously. On the other hand, with increasing SWNT concentration, the material experiences decreased exciton formation due to both the electrically percolated SWNT networks and the increase in quenching of the luminescence emerging from photo or electrical stimuli, and resulting in lower photoluminescence. The optimal luminescence occurs at intermediate concentrations of SWNT due to the combination of all of these mechanisms with the trapping effect dominating at low SWNT concentration and the quenching and exciton suppression dominating at high SWNT concentrations. Overall device failure, however is brought on by carbonization of the polymer, leading to observable dark spots as well as possible gas bubble formation and subsequent delamination. With the relatively high current density in these devices, the presence of bubbles is likely due to the formation of gases in the organic layers as a result of Joule heating.[4,5] Though these experiments suggest the radical scavenging abilities of the SWNTs, it must be noted that exciton population-dependent degradation routes were not controlled for. This is relevant in the case of the pure polymer where the EL intensity was

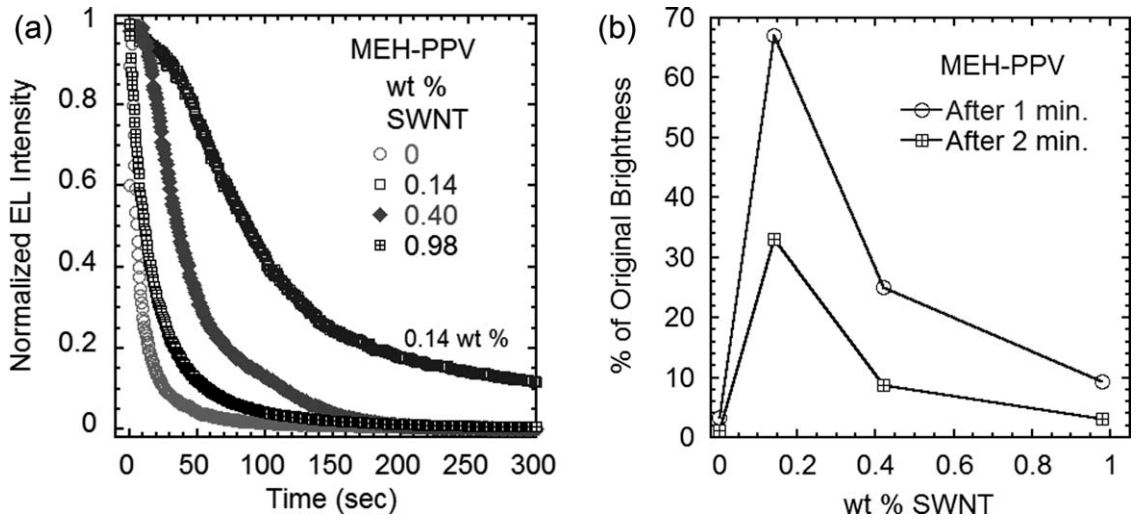

FIGURE 7 The time dependence of the EL intensity for an ITO/PEDOT:PSS/MEH-PPV/Al OLED at a constant potential of 6 V. After 1 min, the brightness of the 0.14 wt % MEH-PPV-SWNT devices is at 67% of its original intensity while the value is reduced to 25% and 9% for the 0.40 and 0.98 wt % devices, respectively. The brightness values for the higher concentration SWNT nanocomposites are still an improvement on the 3.4% remaining brightness of the pure polymer device. After 2 min, the pure and increasingly SWNT-loaded devices bear 1.1, 33, 8.7, and 3.1% of their original brightness.

higher than that for the composites, which quench excitons at levels commensurate with the nanoparticle loading.

CONCLUSIONS

Varying concentrations of dispersed SWNTs were incorporated into three PPV derivatives, namely MEH-PPV, MEH-PPCNV, and DH-PPCNV. Both the electro and photoluminescence properties of the nanocomposites and their applicability as the emissive layer in OLED devices were characterized. The trends observed were qualitatively similar for the nanocomposites based on three different PPV derivative polymers. We found that the dispersed SWNTs affect two competing aspects of device performance: charge transport and exciton dissociation at the SWNT–polymer interface. The *I–V* curves and the current turn-on potentials showed that increased addition of SWNTs improved the conductivity through the fabricated devices and extended the region of Ohmic behavior. However, an undesired increase in the EL turn-on voltage is observed as well as a decrease in the subsequent rate of EL increase with increasing potential difference for the nanocomposites. This result is attributed to the observed photoluminescence quenching by the SWNTs as well as a change in the charge-carrier pathways supported by other studies. The photoluminescence studies on the nanocomposite demonstrated that at higher SWNT loadings it is likely that the interfacial exciton dissociation becomes dominant, observed as quenching of the PL study and diminished EL performance in the OLED devices. Lifetime measurements revealed overall improvement, most likely due to antioxidant effects of the SWNTS. However, it was observed that above a threshold concentration of SWNTs, the percolative nanoparticle network begins to make an impact on the brightness of the devices and gives the impression that the EL of the devices is degrading faster with more SWNTs. Previous work has shown improved lifetimes and lower electroluminescent turn-on voltages in PPV/SWNT nanocomposites; however, the SWNT concentrations presented were lower than those used in this study, indicating that perhaps there is a limit to the benefits of SWNT inclusions in OLED applications. However, the behavior observed with the addition of the SWNTs can be used to optimize the use of nanoparticles in polymer-based photovoltaic devices.

ACKNOWLEDGMENTS

The authors gratefully acknowledge the support of the Texas Institute for Intelligent Bio-Nano Materials and Structures for Aerospace Vehicles, funded by NASA Cooperative Agreement No NCC-1-02038, the National Science Foundation (CMMI-0708096), and the Texas Center for Superconductivity. Authors thank Dr. Timothy Fulghum and Dr. Akira Baba for their assistance in the device performance measurements and Mr. Bhavin Parekh for some early insight into the preparation and performance of such SWNT-based PPV devices.

REFERENCES AND NOTES

1 Friend, R. H.; Gymer, R. W.; Holmes, A. B.; Burroughes, J. H.; Marks, R. N.; Taliani, C.; Bradley, D. D. C.; Santos, D. A. D.; Bredas, J. L.; Logdlund, M.; Salaneck, W. R. *Nature* **1999,** *397*, 121–128.

2 Thompson, M. *MRS Bull.* **2007,** *32*, 694–701.

3 Winey, K. I.; Kashiwagi, T.; Mu, M. *MRS Bull.* **2007,** *32*, 348–353.

4 Czerw, R.; Carroll, D. L.; Woo, H. S.; Kim, Y. B.; Park, J. W. *J. Appl. Phys.* **2004,** *96*, 641–644.

5 Savvate'ev, V. N.; Yakimov, A. V.; Davidov, D.; Pogreb, R. M.; Neumann, R.; Avny, Y. *Appl. Phys. Lett.* **1997,** *71*, 3344–3346.

6 Burrows, P. E.; Bulovic, V.; Forrest, S. R.; Sapochak, L. S.; McCarty, D. M.; Thompson, M. E. *Appl. Phys. Lett.* **1994,** *65*, 2922–2924.

7 (a) Hale, G. D.; Jackson, J. B.; Shmakova, O. E.; Lee, T. R.; Halas, N. J. *Appl. Phys. Lett.* **2001,** *78*, 1502–1505; (b) Bartelmess, J.; Ehli, C.; Cid, J. J.; Garcia-Iglesias, M.; Vazquez, P.; Torres, T.; Guldi, D. M. *Chem. Sci.* **2011,** *2*, 652–660; (c) Ferrance, J. P.; Meissner, K. E.; Pettit, J. W. *J. Nanoparticle Res.* **2010,** *12*, 405–415.; (d) Chu, S. S.; Yi, W. H.; Wang, S. F.; Li, F. M.; Feng, W. K.; Gong, Q. H. *Chem. Phys. Lett.* **2008,** *451*, 116–120.

8 Neef, C. J.; Ferraris, J. P. *Macromolecules* **2000,** *33*, 2311–2314.

9 Brown, K. E.; Breez, A. J.; Rumbles, G.; Gregg, B. A.; Parilla, P. A.; Perkins, J. D.; Tillman, H.; Horhold, H.-H.; Ginley, D. S. *Photovoltaic Specialists Conference, 2002. Conference Record of the Twenty-Ninth IEEE, New Orleans, Louisiana* **2002,** 1186–1189.

10 Georgakilas, V.; Kordatos, K.; Prato, M.; Guldi, D. M.; Holzinger, M.; Hirsch, A. *J. Am. Chem. Soc.* **2002,** *124*, 760–761.

11 Hirsch, A. *Angew. Chem. Int. Ed.* **2002,** *41*, 1853–1859.

12 (a) Krishnamoorti, R.;*MRS Bull.* **2007,** *32*, 341–347; (b) Clark, M. D.; Subramanian, S.; Krishnamoorti, R. *J. Colloid Interface Sci.* **2011,** *354*, 144–151; (c) Chatterjee, T.; Lorenzo, A. T.; Krishnamoorti, R. *Polymer* **2011,** *52*, 4938–4946; (d) Kumar, S. K.; Krishnamoorti, R. *Annu. Rev. Chem. Biomol. Eng.,* **2010,** *1*, 37–58; (e) Clark, M. D.; Krishnamoorti, R. *J. Phys. Chem. C* **2009,** *113*, 20861–20868; (f) Chatterjee, T.; Krishnamoorti, R. *Macromolecules* **2008,** *41*, 5333–5338; (g) Chatterjee, T.; Jackson, A.; Krishnamoorti, R. *J. Am. Chem. Soc.* **2008,** *130*, 6934–6935.

13 Ausman, K. D.; Piner, R.; Lourie, O.; Ruoff, R. S.; Korobov, M. *J. Phys. Chem. B* **2000,** *104*, 8911–8915.

14 Star, A.; Stoddart, J. F. *Macromolecules* **2002,** *35*, 7516–7520.

15 Zhao, W.; Song, C.; Pehrsson, P. E. *J. Am. Chem. Soc.* **2002,** *124*, 12418–12419.

16 Israelachvili, J. N. Intermolecular and Surface Forces. Academic Press; 3rd edition, New York **2006.**

17 Thess, A.; Lee, R.; Nikolaev, P.; Dai, H.; Petit, P.; Robert, J.; Xu, C.; Lee, Y. H.; Kim, S. G.; Rinzler, A. G.; Colbert, D. T.; Scuseria, G. E.; Tomanek, D.; Fischer, J. E.; Smalley, R. E. *Science* **1996,** *273*, 483–487.

18 Matarredona, O.; Rhoads, H.; Li, Z.; Harwell, J. H.; Balzano, L.; Resasco, D. E. *J. Phys. Chem. B* **2003,** *107*, 13357–13367.

19 Yurekli, K.; Mitchell, C. A.; Krishnamoorti, R. *J. Am. Chem. Soc.* **2004,** *126*, 9902–9903.

20 Banerjee, S.; Hemraj-Benny, T.; Wong, S. S. *Adv. Mater.* **2005,** *17*, 17–29.

21 Herrero, M. A.; Prato, M. *Mol. Cryst. Liq. Cryst.* **2008,** *483*, 21–32.

22 Bahr, J. L.; Yang, J.; Kosynkin, D. V.; Bronikowski, M. J.; Smalley, R. E.; Tour, J. M. *J. Am. Chem. Soc.* **2001,** *123*, 6536–6542.

23 Hirsch, A.; Vostrowsky, O. *Funct. Mol. Nanostruct.* **2005,** *245*, 193–237.

24 Holzinger, M.; Vostrowsky, O.; Hirsch, A.; Hennrich, F.; Kappes, M.; Weiss, R.; Jellen, F. *Angew. Chem. Int. Ed.* **2001,** *40*, 4002–4005.

25 Fournet, P.; Coleman, J. N.; Lahr, B.; Drury, A.; Blau, W. J.; O'Brien, D. F.; Horhold, H. H. *J. Appl. Phys.* **2001,** *90*, 969–975.

26 Kim, J.-Y.; Kim, M.; Choi, J.-H. *Synth. Met.* **2003,** *139*, 565–568.

27 Kim, J. Y.; Kim, M.; Kim, H. M.; Joo, J.; Choi, J. H. *Opt. Mater.* **2003,** *21*, 147–151.

28 Parekh, B. P.; Tangonan, A. A.; Newaz, S. S.; Sanduja, S. K.; Ashraf, A. Q.; Krishnamoorti, R.; Lee, T. R. *Macromolecules* **2004,** *37*, 8883–8887.

29 Mitchell, C. A.; Krishnamoorti, R. *Macromolecules* **2007,** *40*, 1538–1545.

30 Saito, R.; Dresselhaus, G.; Dresselhaus, M. S. *Carbon* **2000,** *38*, 169–174.

31 Taranekar, P.; Abdulbaki, M.; Krishnamoorti, R.; Phanichphant, S.; Waenkaew, P.; Patton, D.; Fulghum, T.; Advincula, R. *Macromolecules* **2006,** *39*, 3848–3854.

32 Kymakis, E.; Alexandou, I.; Amaratunga, G. A. J. *Synth. Met.* **2002,** *127*, 59–62.

33 Kymakis, E.; Amaratunga, G. A. J. *Appl. Phys. Lett.* **2002,** *80*, 112–114.

34 Kymakis, E.; Amaratunga, G. A. J. *Rev. Adv. Mater. Sci.* **2005,** *10*, 300–308.

35 Riggs, J. E.; Guo, Z.; Carroll, D. L.; Sun, Y. P. *Phys. A* **1998,** *67*, 29–33.

36 Yang, C.; Wohlgenannt, M.; Vardeny, Z. V.; Blau, W. J.; Dalton, A. B.; Baughman, R.; Zakhidov, A. A. *Phys. Rev. B: Condens. Matter* **2003,** *338*, 366–376.

37 Lee, K. W.; Lee, S. P.; Choi, H.; Mo, K. H.; Jang, J. W.; Kweon, H.; Lee, C. E. *Appl. Phys. Lett.* **2007,** *91*, 023110.

38 Mulazzi, E.; Perego, R.; Aarab, H.; Mihut, L.; Lefrant, S.; Faulques, E.; Wéry, J. *Phys. Rev. B* **2004,** *70*, 155206.

39 Xu, Z.; Wu, Y.; Hu, B.; Ivanov, I. N.; Geohegan, D. B. *Appl. Phys. Lett.* **2005,** *87*, 263118.

40 Woo, H. S.; Czerw, R.; Webster, S.; Carroll, D. L.; Ballato, J.; Strevens, A. E.; O'Brien, D.; Blau, W. J. *Appl. Phys. Lett.* **2000,** *77*, 1393–1395.

41 Woo, H. S.; Kim, Y. B.; Czerw, R.; Carroll, D. L.; Ballato, J.; Ajayan, P. M. *J. Korean Phys. Soc.* **2004,** *45*, 507–511.

42 Tada, K.; Onoda, M. *Adv. Funct. Mater.* **2004,** *14*, 139–145.

43 Krusic, P. J.; Wasserman, E.; Keizer, P. N.; Morton, J. R.; Preston, K. F. *Science* **1991,** *254*, 1183–1185.

44 Watts, P. C. P.; Fearon, P. K.; Hsu, W. K.; Billingham, N. C.; Kroto, H. W.; Walton, D. R. M. *J. Mater. Chem.* **2003,** *13*, 491–495.